J Bone Miner Metab (2005) 23:302–308
DOI 10.1007/s00774-005-0603-x

ORIGINAL ARTICLE

Hiroki Yokota · Shigeo M. Tanaka

Osteogenic potentials with joint-loading modality

Received: July 1, 2004 / Accepted: February 9, 2005

Abstract Osteogenic potentials with a novel joint-loading modality were examined, using mouse ulnae as a model system. Load-induced deformation of rigid bone is known to generate interstitial fluid flow and stimulate osteogenesis. However, in most of the previous studies, loads were applied to cortical bone. In the current study, we addressed the question of whether deformation of the epiphysis underneath the joint would enhance bone formation in the epiphysis and the diaphysis. In order to answer the question, we applied lateral loads to a mouse elbow and conducted a bone histomorphometric analysis, as well as measurements of strains and streaming potentials. Compared to the no-loading control, the histomorphometric results showed that 0.5-N loads, applied to the elbow at 2 Hz for 3 min/day for 3 consecutive days, increased the mineralizing surface (two- to threefold), the rate of mineral apposition (three- to fivefold), and the rate of bone formation (six- to eightfold) in the ulna. Strain measurements indicated that strains of around 30 μstrain, induced with the joint-loading modality, were under the minimum effective strain of around 1000 μstrain, which is considered necessary to achieve strain-driven bone formation. To evaluate the induction of fluid flow with the joint-loading modality, streaming potentials were measured in separate experiments, using mouse femurs ex vivo. We found that the streaming potentials correlated to the magnitude of the load applied to the epiphysis ($r^2 = 0.92$), as well as the flow speed in the medullary cavity ($r^2 = 0.93$). Taken together, the findings of the current study support the idea of joint-loading driven osteogenesis, through a mechanism that involves the induction of fluid flow in cortical bone.

Key words Mechanical loading · Elbow · Bone formation · Streaming potential · Strain

H. Yokota · S.M. Tanaka
Department of Anatomy and Cell Biology, Indiana University School of Medicine, Indianapolis, IN, USA

H. Yokota
Department of Biomedical Engineering, Indiana University – Purdue University Indianapolis, Indianapolis, IN, USA

S.M. Tanaka (✉)
Graduate School of Natural Science and Technology, Kanazawa University, Kakuma-machi General Education Hall 517, Kanazawa 920-1192, Japan
Tel. +81-76-264-5847; Fax +81-76-234-4170
e-mail: shigeo@t.kanazawa-u.ac.jp

Introduction

The goal of this study was to evaluate the role of lateral loads, applied to the epiphysis underneath the joint, in elevating bone formation in the epiphysis and the diaphysis. Preventing bone loss is a critical health issue, particularly in aging populations [1], as well as in astronauts in space [2]. In order to minimize decreases in bone mass, one of the effective treatments is to use mechanical loading. In animal studies, loads are usually applied to generate strain in hard cortical bone. A minimum effective strain of around 1000 μstrain is reported to be necessary for load-driven bone adaptation, and interstitial fluid flow induced by strain in situ is considered to activate the genes responsible for osteogenic responses [3]. Load-driven fluid flow has been detected ex vivo and in vivo [4,5], and in vitro studies show that flow shear stimulates the proliferation and differentiation of osteoblasts [6–8] and osteocytes [9,10].

We addressed the question of whether lateral deformation of the epiphysis underneath the joint would enhance bone formation in the epiphysis and the diaphysis with an in situ strain smaller than the minimum effective strain. Although loads applied to the joint would be absorbed and attenuated in soft connective tissues surrounding the epiphysis [11,12], we proposed a novel joint-loading modality, based on the following considerations. First, trabecular bone in the epiphysis is less stiff in the lateral direction than in the axial direction and, therefore, lateral loads to the elbow may effectively deform the epiphysis of the ulna. Deformation of the epiphysis may then induce fluid flow in the ulnar diaphysis in cortical bone, and load-induced fluid

flow may enhance bone formation in the epiphysis and the diaphysis.

In the current study, we mainly focused on bone histomorphometric analysis in order to examine the osteogenic potential of the novel joint-loading modality. A piezoelectric mechanical loader [13] was employed to apply lateral loads to a murine elbow for 3 min per day for 3 consecutive days. In order to evaluate the in situ strain in cortical bone and compare it to the minimum effective strain, bone strains were measured at three locations on the periosteal surface along the ulnar midshaft. We also evaluated streaming potentials, in response to lateral loads on the epiphysis, in experiments using murine femurs ex vivo. We show, in this report, that loads applied to the elbow can enhance bone formation in the epiphysis and the diaphysis with an in situ strain as small as around 30 μstrain.

Materials and methods

Mechanical loading

In this study, seven C57BL/6 mice (female, 14 weeks old) with a body weight of around 20 g were used. The mice were mask-anesthetized using 2% isoflurane. In order to examine the efficacy of the joint-loading modality, loads were applied to the elbow in a lateral-medial direction with a piezoelectric loader [13] (Fig. 1) for 3 min per day for 3 consecutive days. The loading force was sinusoidal, at 2 Hz, with a peak-to-peak amplitude of 0.5 N. The load was applied to the right arm, and the left arm was used as the non-loading control. To position the elbow properly for the loading experiment, the upper end of the loading rod and the lower end of the supporter (nylon screw) were designed to form a pair of semispherical cups. The elbow was immobilized in the cups, where the medial and the lateral epicondyles of the humerus, together with the ulnar epiphysis, were confined. The forearm was aligned parallel to the cantilever so as to maintain the loading configurations during the experiment. The tip of the loader had a contact area of 4 mm in diameter. In order to avoid local stress concentrations between a joint and the loader, the surface of the loader was covered with a silicon rubber sheet.

The loader consisted of four bimorph-type piezoelectric actuators (LPD12060X; Megacera, Saitama, Japan). A voltage signal was sent through a 16-bit data-acquisition board (PCI-6052E; National Instruments, Austin, TX, USA) and a piezo-driver (model PZD 700-L; Trek, New York, NY, USA). Each actuator was able to generate up to 1.5 N, and the maximum stroke without any load was 2 mm. A strain gauge (CEA-06-062UW; Vishay Measurements Group, Raleigh, NC, USA) on a cantilever detected the applied force, and an eddy-current sensor (DT-110-S-U3-A-C3; Micro-Epsilon Messtechnik, Ortenburg, Germany) was used to measure displacement of the loading rod. Using the force measurement signal, the loader was feedback-controlled at 250-μs intervals.

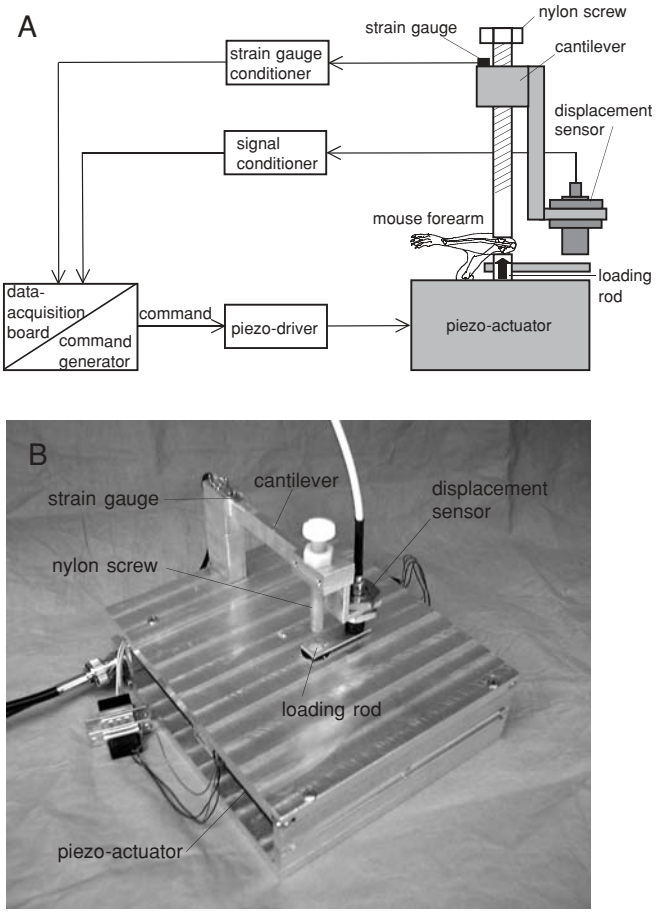

Fig. 1. Piezoelectric mechanical loader used in the study. **A** Systems diagram of the piezoelectric mechanical loader with a signal flow. **B** Systems configuration, including a piezo-actuator, a loading rod and a supporter (nylon screw), a cantilever with a strain gauge, and a displacement sensor

Histomorphometry

A saline solution of 0.05 ml containing 1% calcein was injected 2 and 6 days after the last loading. Ulnae were harvested 13 days after the loading, and the harvested ulnae were fixed in 10% formalin for 2 days. The samples were embedded in methyl methacrylate, after dehydration by immersion in a series of ethanol solutions. Transverse sections of 50 μm in thickness were cut at 1.0, 2.5, and 4.5 mm distal from the elbow, and ground to around 20 μm in thickness. Using the Bioquant semiautomatic digitizing system (R&M Biometrics, Nashville, TN, USA), three morphometric parameters: mineralizing surface (MS/BS), mineral apposition rate (MAR; μm/day), and bone formation rate (BFR/BS; $\mu m^3/\mu m^2$ per year) were determined on periosteal surfaces, where MS = sum of the length of the double-labeled perimeter and half of the single-labeled perimeter; BS = total length of the perimeter; MAR = average radial distance between the two labels per day; and BFR/BS = MS/BS × MAR [14]. Histomorphometric analysis for trabecular bone was performed at a site 1.0 mm distal from the loading

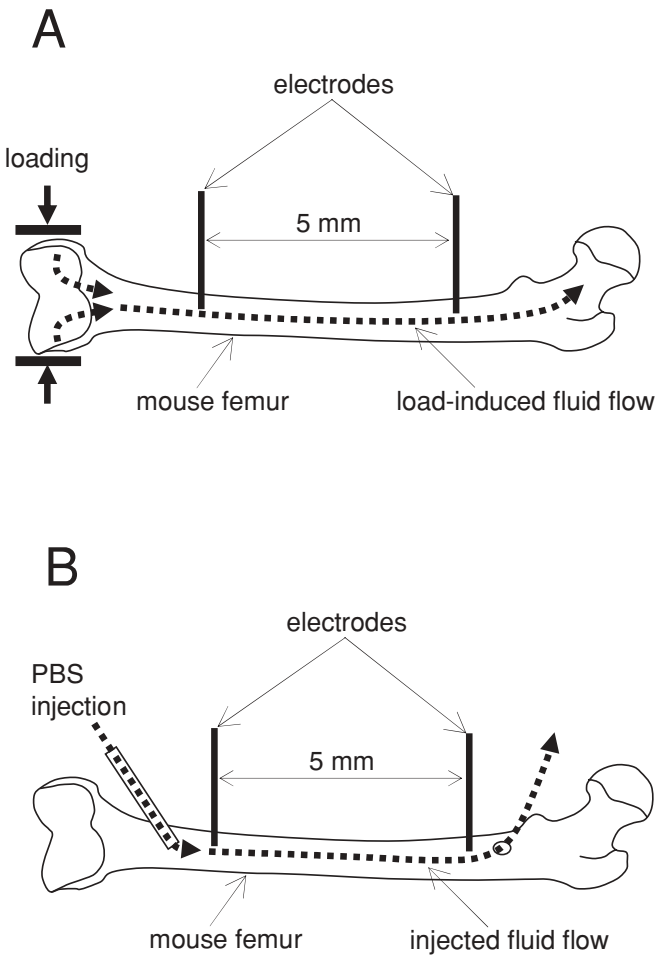

Fig. 2. Schematic diagram of system used for measuring streaming potentials in a murine femur ex vivo. **A** Measurement of streaming potentials in response to lateral loads applied to the femoral distal epiphysis. The voltage differences between the two silver-plated copper electrodes were measured in the medullary cavity. **B** Measurement of reference streaming potentials under conditions of fluid flow with a known flow speed. Phosphate-buffered saline (*PBS*) solution was injected externally to the medullary cavity

site. In addition to the above parameters, the volume of trabecular bone (BV/TV, %) was determined in a cross section, where BV = total area of trabecular bone, and TV = total area of marrow cavities including trabecular bone.

Streaming potential

Bone formation can be stimulated by the induction of fluid flow in cortical bone [15], and the streaming potential serves as an indicator of fluid flow [16]. The periosteal surface of a mouse femur was dissected free of muscles and kept moist with a phosphate-buffered saline solution (PBS, pH 7.5). Two holes, with diameters of around 0.5 mm, were drilled through the cortex on the anterior surface of the midshaft. Bone marrow in the medullary cavity was flushed out, and the cavity was filled with PBS. Two electrodes were inserted, 5 mm apart from each other, into the femoral medullary cavity (Fig. 2). The electrodes were silver-plated copper wires with a diameter of 0.1 mm. They were inserted through the holes, and the holes were sealed with cyanoacrylate glue (M-Bond 200; Vishay Measurements Group). Using the piezoelectric loader, sinusoidal loads (0.5 N to 9 N peak-to-peak) were applied to the femoral distal epiphysis at 2 Hz in a lateral-medial direction, and the voltage signal from the electrodes was recorded at 250-μs intervals (Fig. 2A). Fast Fourier Transform was conducted to extract the signal synchronous to the loading frequency at 2 Hz. Ten femurs were used in the experiment, and the spectrums obtained from fifty loadings were accumulated and averaged.

To calibrate the measurement system, we examined the streaming potentials induced by fluid flow with a known speed. One ml of PBS was injected into the medullary cavity through an inlet hole on the anterior midshaft, using a syringe with a 20-G needle, and the solution was drained from an outlet hole (Fig. 2B). The voltage signal was analyzed with a digital oscilloscope (TDS 2014; Tektronix, Beaverton, OR, USA), and the flow speed (u; mm/s) in the solution was estimated, according to the equation:

$$u = V/A/t \quad (1)$$

where "V" is the volume of the injected solution (1 ml), "A" is the cross-sectional area of the medullary cavity (around 1 mm^2), and "t" is the time spent to inject the solution.

Bone strain

A mouse forearm was dissected, and the medial periosteal surface of the ulna was exposed. A strain gauge – single-element type 0.7 mm in width and 4.0 mm in length (model EA-06-015DJ-120; Vishay Measurements Group) – was fixed to the medial periosteal surface with cyanoacrylate glue 2.5 mm or 4.5 mm from the loading center on the elbow (Fig. 3A). The elbow was loaded at 2 Hz with 0.5-N peak-to-peak force, using the piezoelectric loader (Fig. 3B). Voltage signals from the strain gauge were sent to the digital oscilloscope via a signal conditioning amplifier (2210; Vishay Measurements Group). Peak voltage was recorded and converted to the actual strain value, using the calibration factor, which was derived from known strains generated in the aluminum cantilever.

Data analysis

In order to examine the statistical significance of differences in the histomorphometric data, analysis of variance (ANOVA) (StatView; version 5.0; SAS Institute, Cary, NC, USA) was conducted, with significance levels of $P < 0.05$; $P < 0.01$; and $P < 0.001$.

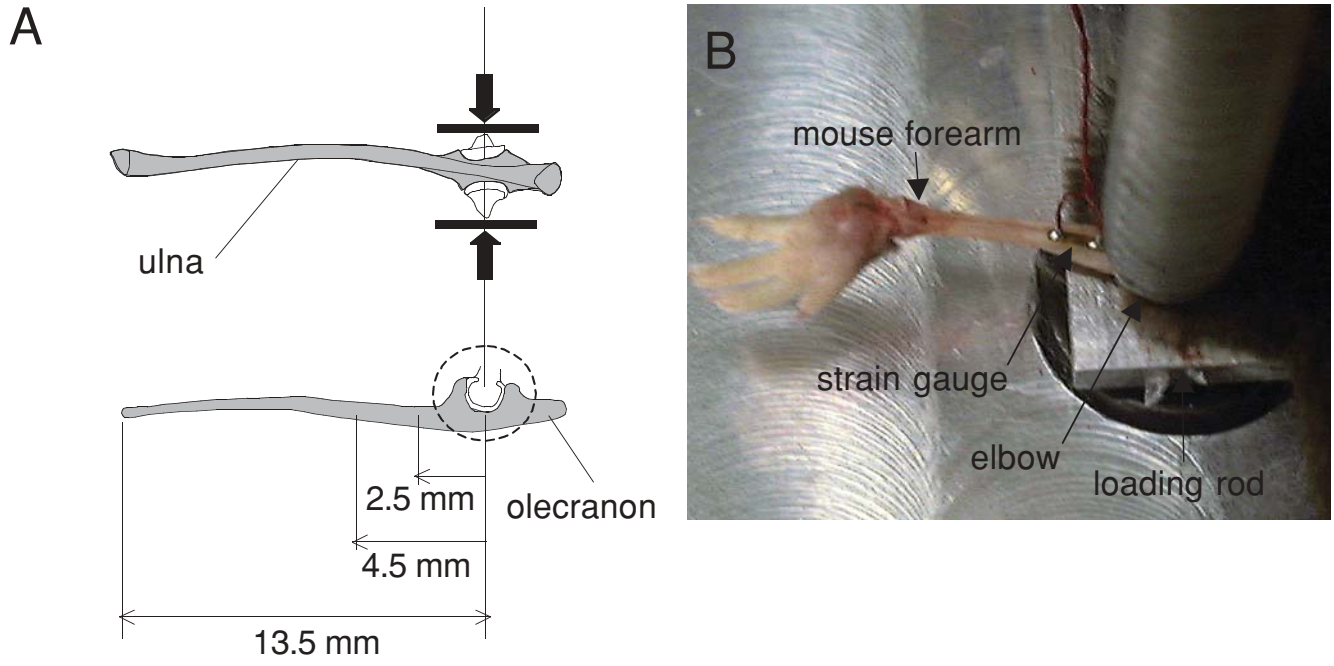

Fig. 3. Measurements of bone strain on a murine ulna ex vivo. **A** Strain measurements were performed on mouse ulnae, 2.5 mm or 4.5 mm from the elbow, in response to lateral loads at 2 Hz with 0.5-N peak-to-peak force (*arrows*). **B** A strain gauge (0.7 mm × 4.0 mm) was glued to the medial periosteal surface of the ulna 2.5 mm from the elbow

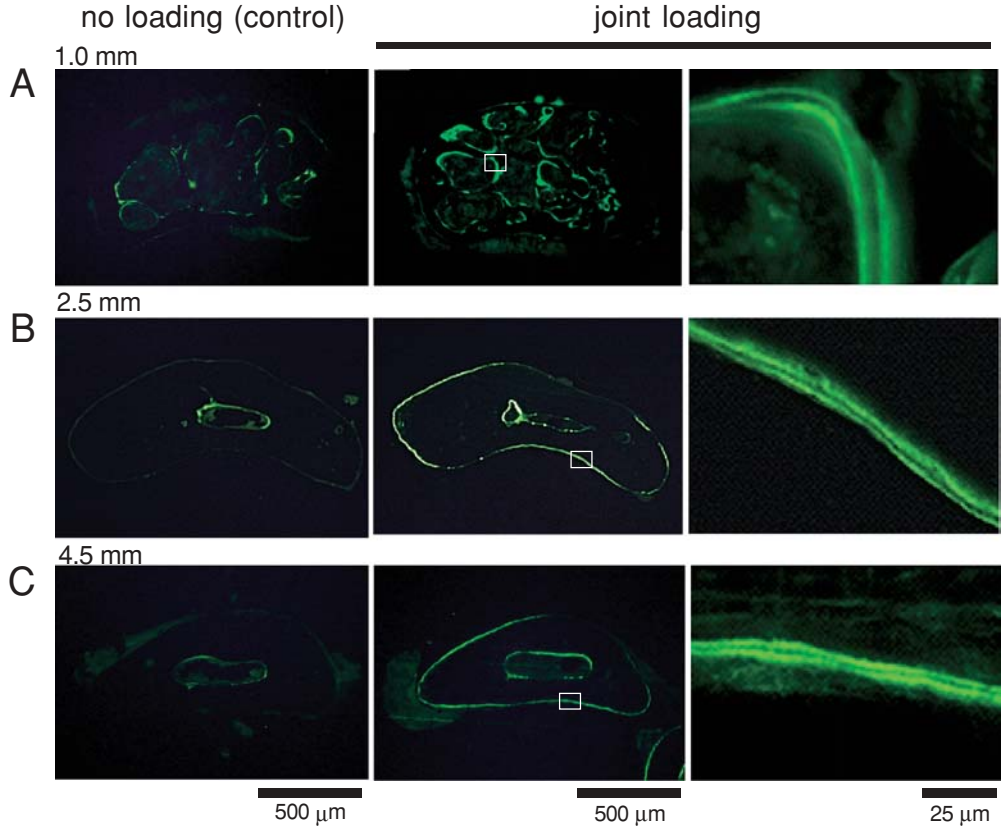

Fig. 4. Cross-sections of the ulnar shafts of control (no loading) and joint-loaded mice. The zoom images on the *far right* show double calcein staining, where the confined area constituted bone newly formed in 4 days. **A** Section of the metaphysis (trabecular bone) 1 mm from the loading center. The light staining outside the periosteal surface is collagen autofluorescence in a tendon of the triceps. **B** Section of the diaphysis (cortical bone) 2.5 mm from the loading center. **C** Section of the diaphysis (cortical bone) 4.5 mm from the loading center

Table 1. Bone histomorphometric parameters

Distance from loading site	TV/BV (%)	MS/BS (%)	MAR (μm/day)	BFR/BS ($\mu m^3/\mu m^2$ per year)
1.0 mm				
Trabecular bone				
No loading (control)	17.0 ± 1.9	33.8 ± 2.0	1.32 ± 0.07	165.0 ± 15.7
Joint loading	23.8 ± 2.2*	44.1 ± 2.3*	1.89 ± 0.11**	306.5 ± 24.0**
Fold change	1.4 ×	1.3 ×	1.4 ×	1.9 ×
Periosteal cortical bone				
No loading (control)		11.7 ± 2.6	0.16 ± 0.10	10.8 ± 7.2
Joint loading		22.4 ± 5.8*	0.75 ± 0.25*	88.8 ± 31.3*
Fold change		1.9 ×	4.7 ×	8.2 ×
2.5 mm				
Periosteal cortical bone				
No loading (control)		10.9 ± 2.1	0.20 ± 0.14	11.5 ± 8.7
Joint loading		34.3 ± 3.7***	0.59 ± 0.16*	90.5 ± 26.9*
Fold change		3.1 ×	3.0 ×	7.9 ×
4.5 mm				
Periosteal cortical bone				
No loading (control)		9.3 ± 1.9	0.16 ± 0.11	9.5 ± 7.1
Joint loading		21.4 ± 5.1*	0.54 ± 0.17*	55.3 ± 20.4*
Fold change		2.3 ×	3.4 ×	5.8 ×

* $P < 0.05$; ** $P < 0.01$; *** $P < 0.001$
Statistically significant differences from no-loading control
Measurements were taken at 1 mm, 2.5 mm, and 4.5 mm distant from the loading site. The values for parameters are shown as means ± SE of seven measurements

Results and discussion

New bone formation induced by joint-loading modality

The histomorphometric analysis of cortical bone at three locations in the ulna revealed significant increases in three bone-formation parameters (Fig. 4 and Table 1). Regardless of the distance from the loading site, the joint-loading modality, used for 3 consecutive days, elevated the amount and the rate of newly formed bone compared to the non-loading control. The mineralizing surface (MS/BS) was increased by 1.9-, 3.1-, and 2.3-fold at sites 1.0, 2.5, and 4.5 mm from the loading site, respectively. The mineral apposition rate (MAR) and bone formation rate (BFR/MS) were elevated by 3.0- to 4.7-fold and by 5.8- to 8.2-fold, respectively. Although the amounts of the increases varied among the three parameters, there were no statistically significant differences for any parameter among the measurement locations. The joint loading also enhanced the formation of trabecular bone. Compared to the finding in the non-loading control, the volume of trabecular bone was elevated by 1.4-fold, with increases of MS/BS (1.3-fold), MAR (1.4-fold), and BFR/MS (1.9-fold).

With the axial ulna-bending modality, which is one of the existing mechanical loading methods to induce bone formation [17], the force required to elevate the rate of bone formation is reported to be 2.3 N [18]. With the joint-loading modality described here, bone formation was enhanced by loads as small as 0.5 N. The results of this study indicate that the joint-loading modality is more effective in inducing bone formation than the axial ulna-bending modality, suggesting the possibility that lateral loads applied to the elbow are a potent inducer of fluid flow in the ulna.

The cross-sectional images of the ulna, together with the data on bone strains, support the notion that enhanced formation of cortical bone was an adaptive response to mechanical stimuli rather than a response associated with wound healing. First, the histological sections clearly showed double-labeled staining on the periosteal surface, with no indication of woven bone, which would frequently be formed in the process of wound healing. Second, unlike the four-point bending modality, where woven bone is formed underneath soft connective tissues, due to bending moment or compressive stress [19], our data on bone strains indicate that the joint-loading modality did not induce mechanical stress comparable to that with the four-point bending modality at the site of new bone formation. Lastly, molecular analysis with the joint-loading modality indicated that no inflammatory responses were evident in the expression or activity of a family of matrix metalloproteinases in connective tissues underneath the loading site (data not shown).

Induction of streaming potentials with the joint-loading modality

Lateral loads, applied to the distal epiphysis of the mouse femur ex vivo, induced streaming potentials. The measured intramedullary streaming potential (ϕ_1, in μV) correlated to the magnitude of the applied force (Fig. 5A), according to the equation:

$$\phi_1 = 7.3 \times \mathrm{F} \left(r^2 = 0.92\right) \quad (2)$$

where "F" = applied force (in N). From Eq. (2), the streaming potential inducible by the joint-loading modality was

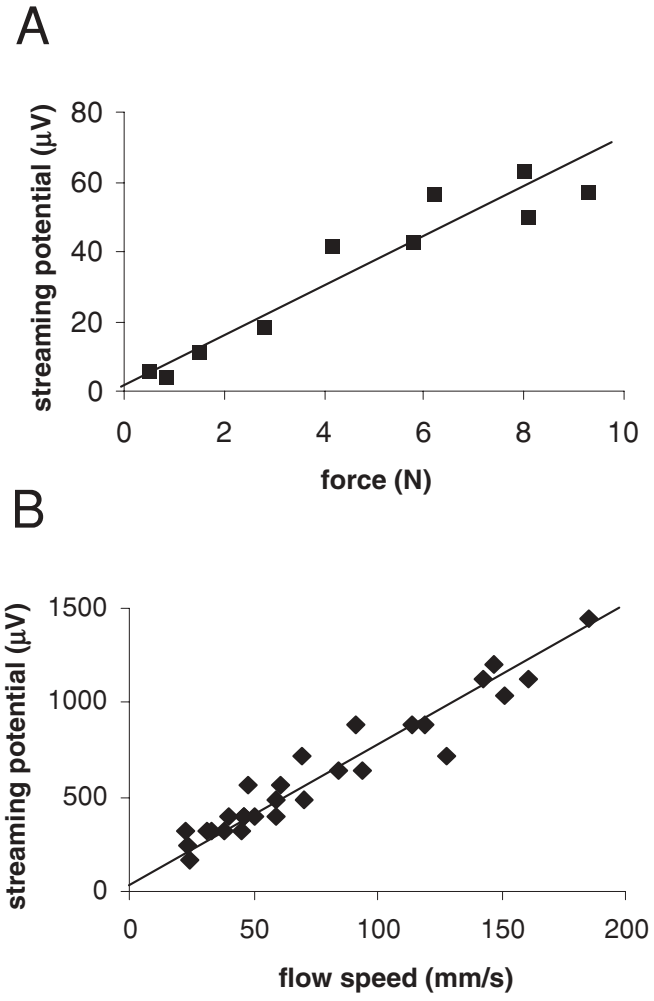

Fig. 5. Streaming potentials in murine femurs. **A** Relationship between streaming potential and the applied force. The linear regression line is $y = 7.3\ x$ ($r^2 = 0.92$). Streaming potential was expressed as the peak-to-peak magnitude of voltage signals. **B** Relationship between streaming potential and the flow speed. The linear regression line is $y = 7.6\ x$ ($r^2 = 0.93$)

estimated as 3.6 μV, with 0.5 N peak-to-peak force. The injection of PBS, at a known fluid speed, into the medullary cavity generated the streaming potential, which was used to establish the relationship of the streaming potential to the flow speed. This reference potential (ϕ_2, in μV) was expressed with the speed of fluid flow (u in mm/s; Fig. 5B) according to the equation:

$$\phi_2 = 7.6 \times \mathrm{u} \left(r^2 = 0.93\right) \quad (3)$$

These data indicate that the magnitude of the streaming potential in the medullary cavity is proportional to the lateral load applied to the joint and the speed of fluid flow. From Eqs. (2) and (3), the speed of the intramedullary fluid flow induced by 0.5-N loads, applied to the knee, is estimated as 476 μm/s. Note that the streaming potential is affected by the dimension of the cavity, the porosity and electrochemical characteristics of cortical bone, and the solution in the cavity; further analysis is necessary to evaluate load-induced fluid flow in the ulna in vivo.

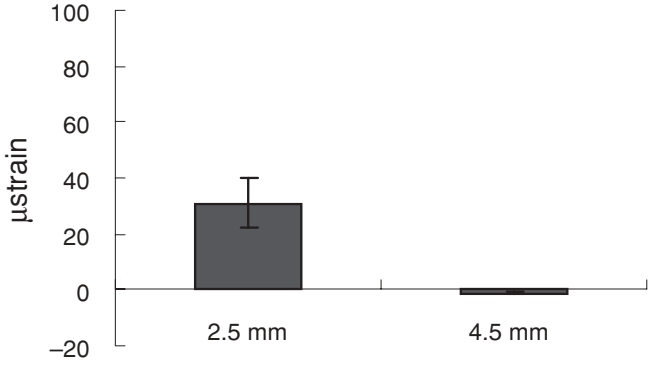

Fig. 6. Bone strain induced by elbow-joint loading. The measured strains were 31 ± 9.1 μstrain at 2.5 mm ($n = 10$) and –1.1 ± 0.7 μstrain at 4.5 mm ($n = 8$) from the elbow-loading center. The lateral loads were applied to the elbow at 2 Hz with a peak-to-peak amplitude of 0.5 N. The values are shown as means ± SE

Bone strain induced by the joint-loading modality

In response to the lateral loads to the elbow, the strain measured in cortical bone was as low as 31 ± 9.1 μstrain at 2.5 mm and –1.1 ± 0.7 μstrain at 4.5 mm, respectively, from the loading center (Fig. 6). Although strains above the minimum effective value at around 1000 μstrain are considered to be necessary to enhance the strain-driven formation of cortical bone in vivo [20,21], the strain observed with the joint-loading modality was considerably smaller than the minimum effective strain. Therefore, we believe that the osteogenic potentials with the elbow-loading modality are not directly caused by in situ strain in cortical bone.

Potential mechanism for bone formation induced by joint loading

Based on the findings of enhancement of bone formation and induction of streaming potentials by the joint-loading modality, a novel mechanism for load-driven fluid flow is suggested, as illustrated in Fig. 7. In the commonly accepted view, bone formation is stimulated by fluid flow induced by the in situ deformation of cortical bone, and this strain-induced fluid flow is considered to trigger the osteogenic responses of osteoblasts and osteocytes. An alternative path for the induction of fluid flow, indicated in the current study, is that lateral deformation of the epiphysis would be able to generate fluid flow in the diaphysis. First, strain either in the diaphysis or the epiphysis was below around 1000 μstrain – the minimum effective strain. Therefore, in situ strain alone is not a direct cause of the observed osteogenic potentials. Second, the joint-loading modality enhanced bone formation on the diaphyseal surfaces more intensively than in the epiphyseal bone, although the in situ strain in the diaphysis was smaller than that in the epiphysis. Based on the above reasons, one interpretation is that fluid flow is induced with the loads applied to the elbow, not only in the epiphysis but also in the diaphysis. In order to further understand the efficacy and the mechanism of induction of fluid flow, it would be of interest to examine osteogenic

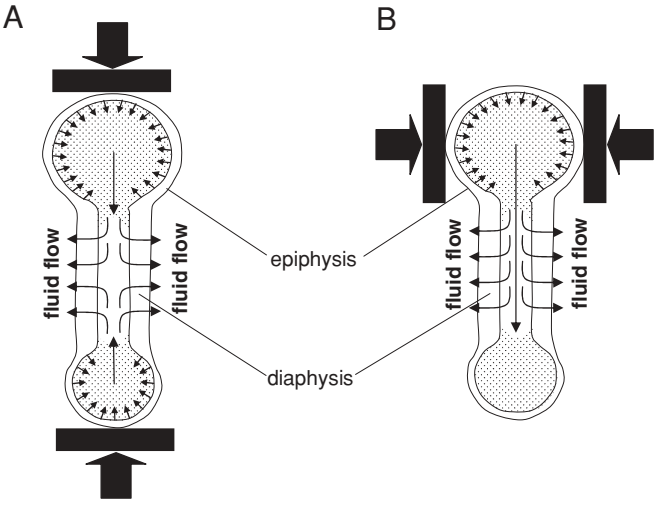

Fig. 7. Schematic illustration of fluid flow in bone. **A** Predicted fluid flow induced by an ulna-bending modality. Two joints are involved in this loading scheme. **B** Predicted fluid flow induced by the joint-loading modality. A single joint (elbow) is involved in this joint-loading modality

potentials in a whole ulna, including more distal locations. Although the measured strain on cortical bone was smaller than the minimum effective strain threshold, it should be noted that the strain at the loading site could have been higher than the measured values in cortical bone. Because the loading site in the current study covered heterogeneous types of tissues, the mechanism of the load-driven fluid flow needs further investigations to determine the quantitative relationship among strain distribution, strain-induced fluid flow, and the morphological parameters involved in the formation of trabecular and cortical bone.

Concluding remarks

Load-driven bone formation is an effective means to strengthen bone and prevent bone loss [22,23]. Most studies have focused on the loads applied to cortical bone and the in situ deformation of hard bone. In this study, we provided evidence that lateral loads applied to the mouse elbow can stimulate bone formation with small in situ strains of around 30 μstrain. Compared to the ulna-bending modality that requires more than a 2-N force for load-driven bone formation, the described joint-loading modality with a 0.5-N force can reduce loading intensity by 75%. In conclusion, osteogenic potentials can be enhanced with the described joint-loading modality without generating in situ strain above the minimum effective strain. The joint-loading modality could be useful in future to develop a novel loading strategy to prevent bone loss in the elderly and in astronauts in space.

Acknowledgments We thank Charles Turner and Imranul Alam for assistance in mechanical loading, and Keith Condon and Hui B. Sun for assistance in bone histomorphometry. This study was supported, in part, by The Whitaker Foundation and NIH R01EB01019.

References

1. Inzerillo AM, Zaidi M (2002) Osteoporosis: trends and intervention. Mt Sinai J Med 69:220–231
2. Droppert PM (1990) The effects of microgravity on the skeletal system – a review. J Br Interplanet Soc 43:19–24
3. Piekarski K, Munro M (1977) Transport mechanism operating between blood supply and osteocytes in long bones. Nature 269: 80–82
4. Knothe Tate ML, Steck R, Forwood MR, Niederer P (2000) In vivo demonstration of load-induced fluid flow in the rat tibia and its potential implications for processes associated with functional adaptation. J Exp Biol 203:2737–2745
5. Tate ML, Knothe U (2000) An ex vivo model to study transport processes and fluid flow in loaded bone. J Biomech 33:247–254
6. Goldstein AS, Juarez TM, Helmke CD, Gustin MC, Mikos AG (2001) Effect of convection on osteoblastic cell growth and function in biodegradable polymer foam scaffolds. Biomaterials 22: 1279–1288
7. Jiang GL, White CR, Stevens HY, Frangos JA (2002) Temporal gradients in shear stimulate osteoblastic proliferation via ERK1/2 and retinoblastoma protein. Am J Physiol Endocrinol Metab 283: E383–389
8. Kapur S, Baylink DJ, William Lau KH (2003) Fluid flow shear stress stimulates human osteoblast proliferation and differentiation through multiple interacting and competing signal transduction pathways. Bone 32:241–251
9. Ajubi NE, Klein-Nulend J, Alblas MJ, Burger EH, Nijweide PJ (1999) Signal transduction pathways involved in fluid flow-induced PGE2 production by cultured osteocytes. Am J Physiol 276:E171–178
10. Klein-Nulend J, van der Plas A, Semeins CM, Ajubi NE, Frangos JA, Nijweide PJ, Burger EH (1995) Sensitivity of osteocytes to biomechanical stress in vitro. FASEB J 9:441–445
11. Derrick TR, Hamill J, Caldwell GE (1998) Energy absorption of impacts during running at various stride lengths. Med Sci Sports Exerc 30:128–135
12. Voloshin A, Wosk J, Brull M (1981) Force wave transmission through the human locomotor system. J Biomech Eng 103:48–50
13. Tanaka SM, Alam IM, Turner CH (2003) Stochastic resonance in osteogenic response to mechanical loading. FASEB J 17:313–314
14. Recker RR (1983) Bone histomorphometry. CRC, Boca Raton
15. Turner CH, Forwood MR, Otter MW (1994) Mechanotransduction in bone: do bone cells act as sensors of fluid flow? FASEB J 8:875–878
16. Qin YX, Lin W, Rubin C (2002) The pathway of bone fluid flow as defined by in vivo intramedullary pressure and streaming potential measurements. Ann Biomed Eng 30:693–702
17. Torrance AG, Mosley JR, Suswillo RF, Lanyon LE (1994) Noninvasive loading of the rat ulna in vivo induces a strain-related modeling response uncomplicated by trauma or periostal pressure. Calcif Tissue Int 54:241–247
18. Robling AG, Turner CH (2002) Mechanotransduction in bone: genetic effects on mechanosensitivity in mice. Bone 31:562–569
19. Robling AG, Burr DB, Turner CH (2001) Skeletal loading in animals. J Musculoskel Neuron Interact 1:249–262
20. Rubin CT, Lanyon LE (1985) Regulation of bone mass by mechanical strain magnitude. Calcif Tissue Int 37:411–417
21. Turner CH, Forwood MR, Rho JY, Yoshikawa T (1994) Mechanical loading thresholds for lamellar and woven bone formation. J Bone Miner Res 9:87–97
22. Bourrin S, Palle S, Genty C, Alexandre C (1995) Physical exercise during remobilization restores a normal bone trabecular network after tail suspension-induced osteopenia in young rats. J Bone Miner Res 10:820–828
23. Oxlund BS, Ortoft G, Andreassen TT, Oxlund H (2003) Low-intensity, high-frequency vibration appears to prevent the decrease in strength of the femur and tibia associated with ovariectomy of adult rats. Bone 32:69–77